THE MISSING PHYSICS IN TRADITIONAL CONVECTION DISCRETIZATION AND A ZERO-DISPERSION-ZERO-DIFFUSION SCHEME

Luiz Eduardo Bittencourt Sampaio, luizebs@vm.uff.br
Universidade Federal Fluminense (UFF) – LMTA/PGMEC
Rua Passo da Pátria 156, bloco E, sala 216, Niterói, RJ, 24210-240, Brazil

Abstract. *In this paper we analyze the main weaknesses of traditional discretization schemes and present a new proposal that achieves zero-dispersion and zero-diffusion for a linear convection transport of a passive scalar in a uniform velocity Þeld. The total error for the new proposal was found to be of the order of the machine precision. The new proposal is also shown to accurately transfer energy around modes as they change their wavelengths in the case of a non-uniform velocity Þeld or in a non-linear convection, irrespective of the proximity of unresolved modes, or the presence of signiÞcant discontinuities in the spectrum resulting from the mesh discretization. This makes it a suitable candidate to several application areas of computational physics, such as aeroacoustics, turbulence, and multiphase SSows. The main ideas that inspired the development of the new scheme are related to a discussion about the necessity of a more suitable error assessment methodology in substitution for the traditional wave number analysis.*
Keywords: *Numerical schemes, convection, dispersion, diffusion, CFD*

1. INTRODUCTION

Several key topics in computational fluid dynamics depend on the accuracy of the convection discretization scheme. Among them are turbulence numerical simulation, computational aeroacoustics (CAA), multiphase flow with the Volume of Fluid (VOF) methodology and its derivations, and others.

In the particular case of turbulence, the Reynolds number is usually high and the convection term is of great importance, as it is the responsible for the non-linearity which generates new frequencies, filling up the spectrum and establishing the well-known energy cascade (Kolmogorov, 1941; Frisch and Kolmogorov, 1995). In Large Eddy Simulations methodology (LES), this energy cascade must be correctly captured, notwithstanding the discrete and finite set of frequencies that are representable by the mesh (Geurts, 2003; Sagaut and Méneveau, 2006). In fact, it is the transfer of energy towards unrepresentable modes – with wavelength shorter than the mesh cut-off – that will play the role of the viscosity dissipation in order to balance out the transfer of energy through the inertial range. Because all traditional convection discretization schemes present spurious behavior at frequencies near the cut-off, some form of artificial damping is always added to the equations in to achieve the required level of dissipation. This artificial solution is usually interpreted as a physical modeling by the scientific community, although some researchers think it should be an explicit physical term, while others reckon it could be somehow incorporated in the numerical scheme as an implicit dissipation. The general consensus, however, is that if the convection discretization is non-dissipative, an additional physical modeling term is required (Morinishi, Lund et al., 1998; Mahesh, Constantinescu et al., 2004).

Contrary to this general consensus, in this author opinion, the need for this additional damping arose only because of imperfections in numerical schemes. If the discretization could exactly represent the resolved-unresolved modes interaction, the energy would naturally SSows towards the subgrid range of the spectrum. Since the mesh is unable to represent modes smaller than cut-off, the end effect would be the disappearance of small turbulent structures. But of course, in order to go without physical modeling, the numerical scheme must be close to perfect in all representable wave numbers, which is a big challenge.

In this paper, we will show that, once a more physically driven approach for error analysis (presented in details in a previous paper on this same congress (Sampaio, 2010)) is chosen instead of the traditional wave number analysis (Lomax, Pulliam et al., 2001), a new low order numerical scheme can be developed that is extremely accurate for the 1-D linear convection in a uniform Þeld. Despite using a very short stencil and being only Þrst order accurate, the computed error is of the order of machine precision. Afterwards, it will be shown that this new scheme is also able to represent the transfer of energy to smaller scales in the subgrid range, without compromising the accuracy of smoother structures.

Because the new scheme is exact for linear convection, with nor dissipative nor dispersive spurious errors, it must be also suitable for Computational Aero Acoustics (CAA), where the delicate interference patterns are very sensitive to errors in both phase and amplitude (Tam, Webb et al., 1993), as well as other areas of computational physics, such as multiphase flows, heat transfer, turbulence with Reynolds Average Navier-Stokes, to cite a few.

2. A NEW PROPOSAL – GRADIENT FIRST ORDER UPWIND

Let us first examine the one-dimensional linear convection in a uniform field, governed by the following equation:

$$\frac{\partial \phi}{\partial t} + u\frac{\partial \phi}{\partial x} = 0\,, \tag{1}$$

where u is the flow velocity convecting ϕ. We shall initially assume u as a uniform and constant field in the following discussion, while the boundaries are considered periodic.

In this case, the solution is simply $\phi(t,x) = \phi_0(x-ut)$, where $\phi_0(x) = \phi(0,x)$ is the initial wave form.

Figure 1 illustrates an initial cosine wave $\phi(0,x) = \cos(kx)$and its convected version, 0.25 seconds later in a uniform velocity field with $u = 1m/s$. The wave number is $k = 2\pi/\lambda$, with $\lambda = 2\Delta x$ in this particular case. Without lost of generality, we set $\Delta x = 1$.

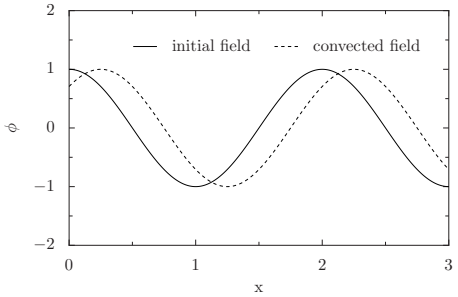

Figure 1. Convection of a cosine scalar field

It is clear that, as the wave is convected one time step (moves to the right), the spatial derivative at the mesh nodes must change from an initial value (equal to zero in this case) to some positive or negative value, depending on the location of the mesh node. That would be the expected result from analytical solution. On the other hand, if one takes a central differences discretization of this initial wave form, the term $\partial\phi/\partial x$ would be zero everywhere, which means, according to Eq. 1, that no changes in ϕ will be noticed. While the literature recommends that *upwinding* should be completely avoided or kept to minimum levels, it is evident that some amount of bias in the discretization is needed to capture the physics of convection. It is not just a question of stability, which is indeed improved by *upwinding*, but more importantly, it seems that, without some form of *upwind* bias, an essential physical aspect of convection would be missed.

Observing the evolution of the wave form, in successive time steps, it is also clear that the spatial derivative to be used in the discretized equation should not be based on simple operations with node values. In the same Figure, the spatial derivatives calculated at $t = 0.5$ would always be zero, no matter how large the computational stencil is. However, from the analytical solution $\phi(t = 0,5,x) = \cos(kx - \pi/2)$, the derivative should be $\partial\phi/\partial x|_{t=0,5} = k\cos(kx)$, which is $\partial\phi/\partial x = 2$ for the even mesh nodes and $\partial\phi/\partial x = -2$ for the odd ones.

If, instead of considering the convection of the cosine wave form, one considers the analytical convection of its piecewise linear reconstruction (after sampling the initial form at mesh nodes), it will be clear that the spatial derivatives should be constant until the wave form has travelled one mesh space (Δx). Right after that, the derivative should change its value (to the opposite sign, in this particular case) to become constant again, until the wave has travelled yet another mesh space. Of course, the fact that the derivative should be kept constant over periods of time and only seldom be updated has to do with the piecewise linear reconstruction. Had a different reconstruction been chosen, like a high order polynomial, the derivative would have to be constantly changing, following the shape of the reconstructed wave.

All the points made above suggest that the spatial derivative should be an independent field, evolving according to its own transport equation. In this case, despite the null ϕ field analytically found at $t = 0.5$, the derivative field would still hold the necessary information to recover the same original shape when the wave reaches the next mesh point (becoming a cosine again). Clearly this points out that the energy will be flowing from the primitive field to its derivative (or gradient in 3-D) back and forth, without losing energy or information. This corresponds to the expected behavior, as there is no energy cascade or no change in the structures wavelength when the velocity field is uniform.

Another interesting observation is that, with traditional schemes, the wave will either disappear after a few time steps (if dissipative schemes like upwind is used) or become so dispersed that will not resemble the original form. The important thing is that once the original form is lost, it can never more be recovered. This is because they were designed with the traditional wave number analysis, which, although very helpful in some situations, is restricted to a time range spanning $[t, t + \Delta t]$.

We will now show a general framework for developing consistent numerical schemes that can present minimum or zero errors, at least for the 1-D linear convection in uniform field. The presentation of the new proposal is split into three subsections, for the sake of clarity: the general transport equations; the reconstruction functions; and the time advancing step, in which discrete solution for the transport equations is found.

2.1 General transport equations

The spatial derivative of Eq. 1 is:

$$\frac{\partial G}{\partial t} + u\frac{\partial G}{\partial x} + \frac{\partial u}{\partial x}G = 0\,. \tag{2}$$

In the complete space of functions, Eq. 2 is redundant as it is derived from Eq. 1 – satisfying the latter automatically implies satisfying the former. However, in a truncated discrete environment, this is not the case, and Eq. 2 provides complementary information to the convective transport of ϕ. This (solving for an independent equation for the derivative) was the key missing link, absent in all previous numerical schemes of the literature.

To isolate the influences of the second and third terms in the left hand side of Eq. 2, we note that the third term becomes zero in a uniform flow field, while the second term becomes zero when ϕ is linear (G is constant).

The second term on the left hand side of Eq. 2 is the convection of G and accounts for the change in the spatial derivative (G) due to the shape of the reconstructed function, upon convection. This term alone has the ability to bring upwind information even if unbiased schemes are used in all spatial derivatives.

2.2 Reconstruction

The reconstruction step aims at rebuilding a continuous function with the limited information available – the fields ϕ and G. We will require that the reconstructed function be continuous, but we will not enforce continuity in its derivatives, to keep the computational costs low.

Contrary to spectral methods, and following the general ideas of Finite Difference/Volume/Elements Methods, the reconstruction will be made in a compact support, where a piecewise interpolation is restricted to a vicinity of each node. Here we will use first order polynomials and the values of ϕ and G at each mesh point.

With the values of ϕ and G at two adjacent mesh nodes, x_j and x_{j+1}, one can find the intersection point $(x_{Int}, \phi(x_{Int}))$ and then reconstruct the function at any location in between these two nodes. The reconstructed field ϕ consists of piecewise linear segments, each of them extending from one intersection point (found between x_j and x_{j+1}) to the next (located between x_{j+1} and x_{j+2}), while the reconstructed G is assumed constant in the same piecewise intervals.

This process can be repeated for every pair of adjacent nodes at a generic time $t = t_m = m\Delta t$ (m is an integer number) so that the reconstructed fields ϕ and G are analytically known everywhere for $t = t_m$.

Equations 1 and 2 can then be advanced from t_m to t_{m+1}, using the last know reconstructed fields as the "initial condition" ($t = t_m$). Generally, for the proposed reconstruction, the second term on the RHS of Eq. 2 is null because of the piecewise linear reconstruction. Only exception is when an intersection point crosses a mesh node location. In this case, by solving the jump condition we find that a simple gradient update is sufficient to represent this crossing. This gradient update is done for each node where the crossing occurs, and can be taken as:

$$G(t_m^+, x_j) = \frac{1}{\Delta x}(\phi_j^m - \phi_{j-1}^m)\,, \tag{3}$$

where $t_m^+ = t_m + \varepsilon$ is the time immediately after the time of the crossing, t_m, with $\varepsilon \to 0$ being an infinitesimal number.

It may happen that the crossing does not happens exactly at a discrete time t_m. The solution for this is easy: it suffices to split the time step (supposedly from t_m to t_{m+1}) in three parts: 1) the first (from t_m to t_J^-) obeys the transport equations (Eqs. 1 and 2); 2) the second is the infinitesimal interval t_J^- to t_J^+, and is when the update (Eq. 3) happens; 3) the third (from t_J^+ to t_{m+1}) again obeys the transport equations (Eqs. 1 and 2).

3. NUMERICAL EXPERIMENTS

In this section, results from a number of simple numerical experiments are presented to allow comparison between the new scheme and more traditional ones.

Since it is not easy to apply a wave number analysis to the new proposal, the numerical tests had to be more exhaustive then usual. The initial wave forms were chosen in such a way that its spectral content includes a certain range of frequencies. By varying some parameters in these initial wave functions, a significant part of the spectrum is covered by the tests, including the most critical region in which $k\Delta x = \pi$. Unlike the requirements set for traditional schemes, which always have to be relaxed and accept inaccuracies at this highest resolvable frequency ($k\Delta x = \pi$), here we really want to be exact in all spectral frequencies, as impossible as it may sound at first. Table 1 lists all test cases with the respective initial wave equations, parameters and simulation conditions.

In Table 1, the parameters have the following meaning: N_{pts} is the number of points in the mesh; t_F is the final time of the simulation (although in some tests intermediate snapshots are also examined); $\Delta x_F/L$ is the convection distance travelled by the wave divided by the total length of the domain – only applicable when the flow field is uniform; x_0, when applicable, is a parameter of the initial field equation controlling the initial position of the wave; r, when applicable, is a

Table 1. Test cases

Test	$u(0,x)$	$\phi(0,x)$	N_{pts}	t_F	$\Delta x_F/L$	dt	x_0	r	λ_c
1a	cte = 1	Eq. 6	50	50	1	0.1	25	$r = 10$	N.A
1b	cte = 1	Eq. 6	50	50	1	0.1	25	$r = 3$	N.A
1c	cte = 1	Eq. 6	50	500	10	0.1	25	$r = 3$	N.A
1d	cte = 1	Eq. 6	50	50	1	0.1	25	$r = 1$	N.A
1e	cte = 1	Eq. 7	120	120	1	0.1	60	$r = 10$	5
1f	cte = 1	Eq. 7	120	120	1	0.1	60	$r = 10$	3
1g	cte = 1	Eq. 7	120	120	1	0.1	60	$r = 10$	2
1h	cte = 1	Eq. 7	120	120	1	0.4	60	$r = 10$	3
1i	cte = 1	Eq. 7	120	120	1	1.0	60	$r = 10$	3

parameter controlling the width of the Gaussian used in the initial condition; and λ_c is the wavelength of the oscillations that are applied to a basic form (Gaussian, for instance). "N.A." stands for Not Applicable.

All test cases consist of a unidimensional mesh with periodic conditions at extremities, so that we can evaluate the deterioration of the solution over long periods of time. Without lost of generality, $\Delta x = 1$ for all tests.

3.1 1-D linear convection

One dimensional linear convection (Eq. 1) is often used as a benchmark test, as it clearly shows the effect of dispersion and diffusion in distorting the original wave form.

This test is specially important for numerical schemes aimed at Computational Aero Acoustics (CAA), and because of that, it is natural to expect that such schemes present optimal performance for this case.

Therefore, in these tests we compare the new proposal with two specially optimized CAA schemes (Tam and Webb, 1993): 1- the Dispersion Relation Preserving (DRP) scheme , with a 7 points spatial stencil and a 4 stage Runge-Kutta in time (referred to as "DRP-7" in the legends); and 2- the 15 points DRP stencil, also with a 4 stage Runge-Kutta (referred to as "DRP-15" in the legends). This may not seem a fair comparison, as the present proposal is only first order in space and second order in time, but actually, as it will be shown, the new scheme performed better. Additionally, a traditional second order central differences scheme with a 4 stage Runge-Kutta time step (referred to as "CD2" in the legends) was also tested to provide a fairer comparison.

For uniform convective velocity, the solution for Eq. 1 is simply $\phi(t,x) = \phi(0, x-ut)$, meaning that the initial shape is preserved as the wave travels by convection. Thus, for a convective distance multiple of the domain length, one expects the new field to be exactly coincident with the initial one, as the boundaries are linked as periodic. That makes it very easy to compare to the analytical solution, and a total error can be calculated by:

$$E(t_p = pL/u) = \sqrt{\frac{1}{N_{pts}} \sum_{j=1}^{N_{pts}} \left[\phi(t_p, x_j) - \phi(0, x_j)\right]^2}\,, \tag{4}$$

where p is an integer number.

This error can be normalized by the square root of the wave energy,

$$E_{norm} = E \left[\frac{1}{N_{pts}} \sum_{j=1}^{N_{pts}} \left[\phi(0, x_j)\right]^2 \right]^{-0.5}\,. \tag{5}$$

Without lost of generality, the velocity is taken as $u = 1m/s$. The Courant number, $\eta = u\Delta t/\Delta x$ is the only parameter in the non-dimensional version of Eq. 1, and will be varied through changes in the time step, Δt.

Table 2 reports the errors found in the tests listed in Tab. 1.

For the first tests ("1a" to "1d"), the initial wave form is a bell-shaped one,

$$\phi = \exp\left[-\log(2.0) \left[\frac{(x - x_0)}{r} \right]^2 \right]\,, \tag{6}$$

where x_0 is the initial location, and r is a parameter controlling the width of the Gaussian.

Greater values of r are easier on the numerical schemes since, by wave number analysis, the spectral content is farther from the critical spatial frequency, as $k\Delta x \ll \pi$. On the other hand, as r becomes smaller, modes with wavelength closer to twice the mesh space begin to appear, which is known to be a problem for all traditional schemes.

Table 2. Normalized errors for test case 1

Test ID	CD2	DRP-7	DRP-15	new proposal
1a	1.84×10^{-2}	9.29×10^{-4}	5.42×10^{-4}	1.09×10^{-15}
1b	4.69×10^{-1}	7.04×10^{-3}	3.58×10^{-4}	1.63×10^{-15}
1c	N.A.	6.53×10^{-2}	3.58×10^{-3}	1.58×10^{-14}
1d	N.A.	4.82×10^{-1}	1.82×10^{-1}	3.98×10^{-15}
1e	N.A.	1.30×10^{0}	2.21×10^{-3}	1.59×10^{-14}
1f	N.A.	1.40×10^{0}	1.47×10^{0}	2.32×10^{-14}
1g	N.A.	1.42×10^{0}	1.05×10^{0}	2.66×10^{-14}
1h	N.A.	N.A.	N.A.	1.33×10^{-14}
1i	N.A.	N.A.	N.A.	1.46×10^{-16}

Three different values of r were tested, as shown in the first four lines of Table 1 (tests "1a" to "1d"). The corresponding normalized errors are shown in Table 2.

A modulated version of the same initial Gaussian is obtained by multiplying Eq. 6 by $\cos(k_c x)$, with $k_c = 2\pi/\lambda_c$, yielding:

$$\phi = \cos(k_c x) \exp\left[-\log(2.0) \left[\frac{(x - x_0)}{r} \right]^2 \right] . \tag{7}$$

The modulation operation (multiplication by the $\cos(k_c x)$) corresponds, in Fourier space, to a shift of the spectrum content, that will now be centered around k_c. A critical condition for all traditional schemes happens when λ_c gets close to $2\Delta x$, as it is the case in tests "1e" through "1i". This initial wave resembles that of an amplitude modulated sound packet, whose carrier wave length is λ_c. One of the biggest challenges faced by modern Computational Aero Acoustics (CAA) is that a small mistake in either amplitude or phase of the numerical solution can significantly spoil the interference pattern at the far field and greatly alter the results.

In all tested cases of this section one can notice the superiority of the new proposal when compared to traditional schemes. The total error was of the order of machine precision, which indicates that the algorithm is virtually exact for these simple test cases.

DRP-7 and DRP-15 have poorer error, specially when the mesh cut-off limit is approached (cases with $r \leq 3$ or $\lambda \leq 3$), as already expected.

A really challenging scenario for the DRP-15 is obtained by setting $\lambda_c = 3$ (test "1f"). The initial wave form is completely lost (Fig. 2) and the error reaches 1.47×10^0 (Table 2). Yet again, the new proposal was exact to 2.3210^{-14}, and this was also the case even if we further decrease the mesh resolution with $\lambda_c = 2$ (test "1g" in Table 2).

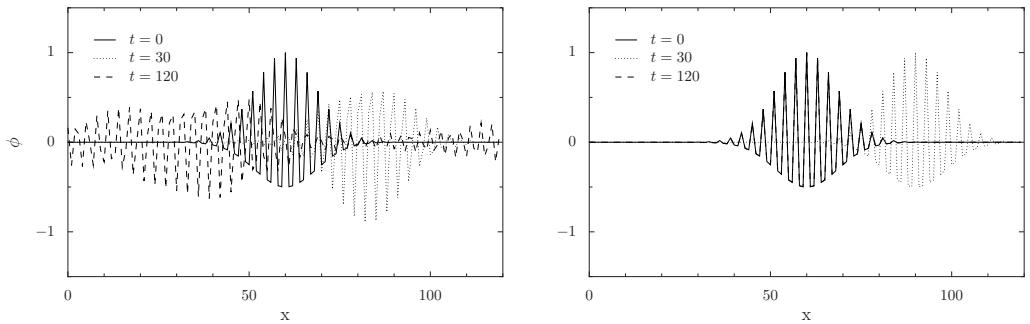

(a) DRP-15 (b) new proposal

Figure 2. Test case 1f: ϕ at $t = 0$, 30 and 120 seconds

The only purpose of tests "1h" and "1i" is to prove that the new scheme also works with other Courant numbers. Test "1h" uses a $dt = 0.4$, resulting in a Courant number $\eta = 0.4$. This was necessary in order to verify that the algorithm also works when the mesh spacing is not a multiple of $u\,dt$, in which case, the jump crossing occurs at the middle of a time step.

Still according to Table 2, exact solutions (1.46×10^{-16}) are also found for situations in which the Courant number is bigger ($\eta = 1$ in test "1i"). The new proposal was not designed, however, for Courant numbers greater than one.

The performance of the new scheme up to now is encouraging, specially considering it is only first order in space and second order in time. Most of the tests were run with low Courant number, in order to isolate the errors due to spatial

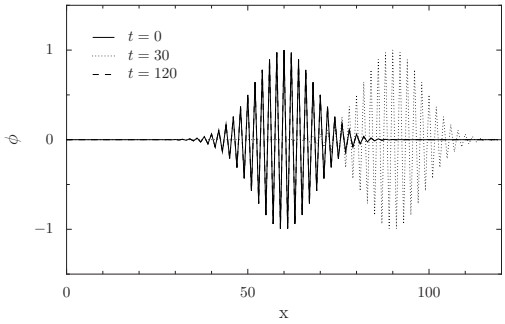

Figure 3. Test case 1h: ϕ at $t = 0$, 30 and 120 seconds

discretization from those due to time discretization. Nonetheless, tests "1h" and "1i" pushed the limits to the extreme Courant allowed by the algorithm, and proved the new proposal is exact in all conditions involving a linear convection equation with uniform flow field. More stringent tests are however needed and are presented in the following sections.

3.2 1-D non-linear convection

The transport equation this time reads

$$\frac{\partial u}{\partial t} + uG = 0\,; \quad G = \frac{\partial u}{\partial x}\,, \tag{8}$$

with G now being the velocity derivative with its own transport equation:

$$\frac{\partial G}{\partial t} + u\frac{\partial G}{\partial x} + G^2 = 0\,. \tag{9}$$

Because of the expansions and contractions experienced when the flow is not uniform, in non-linear phenomena such as turbulence, there is generally some form of energy transfer between different scales. It is, therefore, very likely that some structures, specially the high oscillations, will disappear as they transfer their energy to unresolved (subgrid) scales. It is important to note, however, that the damping of small structure may not mean that the numerical scheme is dissipative. It is possible that this damping are just the natural consequence of accurately capturing the changes in the wavelengths, with their final value falling out of the discrete set that can be represented by the mesh. This means that, with a good numerical scheme, it is theoretically possible to numerically simulate turbulence direct cascade of energy without making use of any subgrid modeling. One must ensure, however, that the small structures damping is not due to spurious dissipation. With the new proposal, this is certainly not that case, as previous uniform flow tests already demonstrated. It remains to be seen if the new proposal can correctly capture this transfer of energy to unresolved modes.

Shock capturing is another non-linear challenge for numerical methods. The shrinking of the wavelengths during the formation of the shock normally generate spurious oscillations in traditional schemes.

Two tests cases were therefore set up in this section. Test"2a" was designed to verify how traditional schemes and the new proposal behave in capturing a shock, using a simple initial condition consisting of piecewise linear ramps. The second test ("2b") was conceived to address the inter-scales energy transfer, in the spectral region close to mesh cut-off. Shock is also present in test "2b", in the final stages of the simulation, so that a more complete picture of the non-linear convection problems is provided.

The initial condition for the velocity field $u(0, x)$, for test "2a", consists of a piecewise linear function connecting the points listed in Table 3.

Table 3. Initial condition for Test 2a – piecewise linear connecting the following points:

$i =$	1	2	3	4	5	6
x_i	1	19	20	60	71	100
y_i	1	1	5	5	1	1

The plot of this initial field is presented in Fig. 4(a)-(h), as a thicker line ($t = 0$).

Results before ($t = 2$) and after shock ($t = 4$) are displayed in the same figure (Fig. 4) in the left and right columns respectively, along with their respective exact (analytical) solutions.

Before shock, all schemes could represent reasonably well the changes in the slopes, although small spurious oscillations were noticed in Fig. 4(a), (c) and (e). The new proposal was, once again, bounded and well behaved (Fig. 4(g)). As

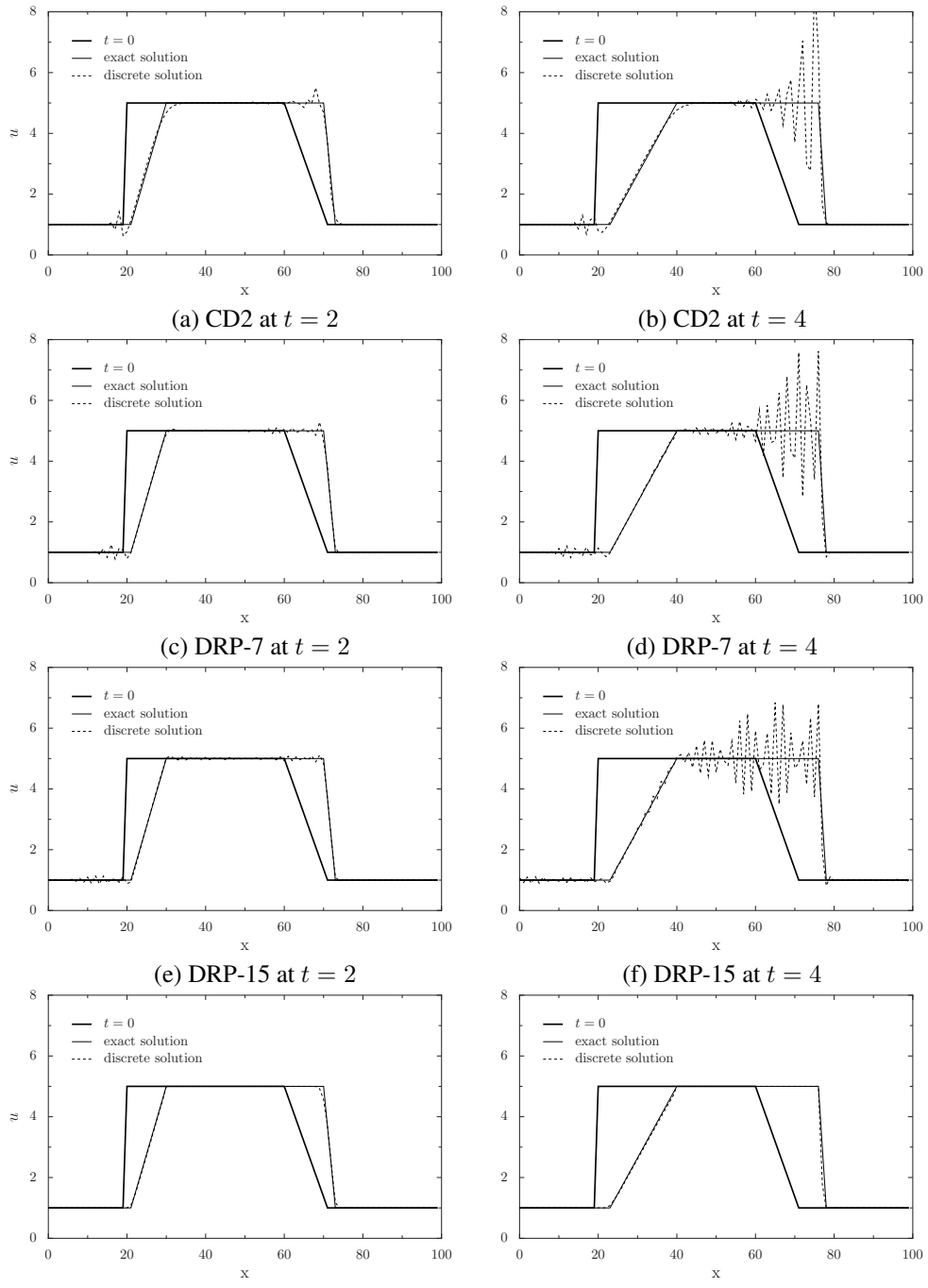

(a) CD2 at $t = 2$ (b) CD2 at $t = 4$

(c) DRP-7 at $t = 2$ (d) DRP-7 at $t = 4$

(e) DRP-15 at $t = 2$ (f) DRP-15 at $t = 4$

(g) new proposal at $t = 2$ (h) new proposal at $t = 4$

Figure 4. Velocity field before ($t = 2$) and after shock ($t = 4$) with DRP-15 and the new proposal.

expected, after the shock all traditional schemes developed severe non-physical oscillationsThe results obtained with the new proposal (Fig. 4(h)) were, however, remarkably accurate, demonstrating that no fixing should be needed when the scheme conception is physically correct.

The last test case of this paper (test "2b") gives us a one dimensional flavor of what can be expected from a more general and complex 3-D turbulence scenario. It aims specifically at checking if the new proposal can correctly capture the transfer of energy to unresolved modes.

For this purpose, test case "2b" was set up with the following initial condition, which contains a high oscillatory content with wavelength $\lambda_c = 2\Delta x$ and a smoother, bell shaped envelope:

$$u(0,x) = 5 + 5\max\left[\cos(k_c x)\exp\left[-\log(2.0)\left[\frac{(x-x_0)}{r}\right]^2\right], 0\right] \ . \tag{10}$$

where, as before, $k_c = 2\pi/\lambda_c$, and the values of u span the range $[5, 10]$ to allow a significant contrast in velocities.

Figure 5 displays the results obtained with two schemes (DRP-15 and the new proposal), as both CD-2 and DRP-7 presented qualitatively the same inaccuracies observed in the DRP-15 . For the sake of visualization, the true initial condition is only used with the new proposal, and are only shown in Fig. 5(b). For all traditional schemes, a filtered version were used instead, which are shown in Fig. 5(a). This was done because the traditional schemes did not correctly damp the high oscillatory initial modes, as in fact they need an additional subgrid model or some kind of artificial dissipation. Moreover, with the dispersion effects, the results were unphysical and difficult to interpret. Therefore, we choose to present, for the traditional schemes, the more reasonable results for a smoother initial wave form, that is obtained after filtering the initial field. It must be mentioned that this choice makes any comparison between a traditional scheme and the new proposal unfair and unfavorable for the latter. The evolution of this filtered field is also shown (dashed lines in the same Figs. 4(a) and (b)), for $t = 0, 1, 3, 5, 7$ and 10 seconds. For these same times, the numerical solutions for the two schemes are presented as solid lines.

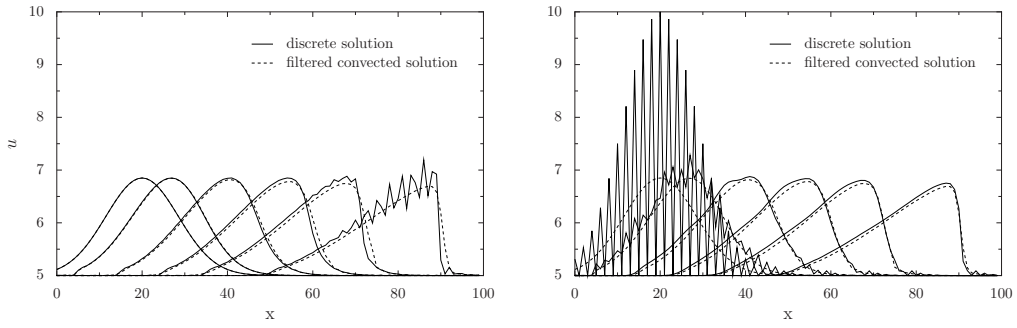

(a) DRP-15 (b) new proposal

Figure 5. Non-linear convection of the initial form described by Eq. 10.

One can observe in Fig. 4(a) that all traditional schemes induce spurious oscillations when shock begins to form (mostly in the last two snapshots in each figure), even being alleviated from the difficulties associated with the true initial wave form (Eq. 10).

The new proposal, on the other hand, not only could cope with a more difficult initial condition, as it also predicted the evolution of the wave without incurring in spurious or unphysical solution. Notice how the initial wave form became successively smoother and closer to the "filtered convected solution" as time goes by. In $t = 1$ (wave peak located at $x \approx 27$), the oscillations were already small, proving that non-linear convection can, in a discretized system, transfer energy to unresolved modes of the spectrum, without any help from subgrid modeling or artificial viscosity. This was also the case with non-uniform flow, and was achieved with a scheme (new proposal) that was virtually exact in an uniform flow environment – no dissipation and no dispersion, with a relative error of 10^{-14}.

Also worth noting is how close the discrete solution became to the "filtered convected solution" in the final stages of the convection ($t = 7$ and 10), which was not the case with traditional schemes. In Large-Eddy Simulations this is highly desirable for the traditional subgrid modeling approach, as they need to act only on a limited band of the spectrum, leaving smoother structures as untouched as possible, as was the case in Fig. 5(d).

4. FINAL REMARKS

The author hopes this work has helped elucidate some controversial topics in the CFD and turbulence simulations community.

First of all, contrary to the general perception, *upwinding* was never the real responsible for the poor performance of numerical simulations. We showed that when a more physically oriented error assessment is employed, it is possible

to design numerical schemes based on first order *upwinding* that are exact at least for the simpler linear convection in uniform flow field, despite being only first order in space and second in time. Optimized traditional schemes used in critical aeroacoustics applications were not able to achieve this, even with a 15 point stencil which implies in a higher computational cost and complexity.

Despite its limitation to transient simulations with Courant number below or equal to one, the results here presented showed that the new proposal is virtually exact for all wave numbers in the spectrum range spanned by the mesh, and for all Courant numbers in the allowed range ($\eta \leq 1$). In fact, the total error (always below 3×10^{-14}), was due to machine precision errors, rather than imperfections in the algorithm itself.

As attested by he results for the non-linear convection, the new proposal can also accurately predict the change of wavelengths or the transfer of energy between modes of different wavelengths, even when the final mode is not resolvable by the mesh. In this latter case, the energy simply disappears, without causing spurious behaviors in neighbor region of the spectrum. This was impossible to achieve with traditional schemes, as all of them presented some imperfection close to the cut-off, which happens to be the most critical region of the spectrum as far as the energy transfer is concerned.

This is specially suited for the representation of the direct energy cascade in a discrete mesh. The new proposal showed that it is possible to transfer energy to unresolved modes in a natural way, and that this should be the responsibility of the discretization scheme alone. One of the encouraging points in the new scheme was that this was done without any further fixing (like normally done with flux limiters or the likes in traditional schemes). Of course, this capability must not be achieved at the cost of degradation of the accuracy in other parts of the spectrum. That is why it was so important to ensure the new proposal was absolutely exact in the whole range of the spectrum, which was basically done with uniform flow linear convection tests.

In the development of this new proposal, two key points were decisive: 1) the development of a transport equation for the derivative (gradient in 3D) of the primitive variable ϕ being convected; 2) a consistent formulation for the reconstruction of ϕ, based only on the knowledge of ϕ and its gradient G. In this paper we focused on presenting a first order version of a bigger family of algorithms and on showing it actually works, but in principle it is possible to extent the concept to higher order reconstructions.

5. ACKNOWLEDGEMENTS

The author gratefully acknowledges the financial support from CNPq.

6. REFERENCES

Frisch, U. and Kolmogorov, A., 1995, Turbulence: the legacy of AN Kolmogorov, Cambridge Univ Pr.

Geurts, B., 2003, Elements of direct and large-eddy simulation, RT Edwards.

Kolmogorov, A., 1941, "Local structure of turbulence in an incompressible fluid for very large reynolds numbers", in "Dokl. Akad. Nauk. SSSR", vol. 30, pp. 299–303.

Lomax, H., Pulliam, T.H., and Zingg, D.W., 2001, Fundamentals of computational fluid dynamics, Scientific Computation, Springer-Verlag, Berlin.

Mahesh, K., Constantinescu, G., and Moin, P., 2004, "A numerical method for large-eddy simulation in complex geometries", Journal of Computational Physics, vol. 197, no. 1, pp. 215–240.

Morinishi, Y., Lund, T., Vasilyev, O., and Moin, P., 1998, "Fully conservative higher order finite difference schemes for incompressible flow", Journal of Computational Physics, vol. 143, no. 1, pp. 90–124.

Sagaut, P. and Méneveau, C., 2006, Large eddy simulation for incompressible flows: an introduction, Springer Verlag.

Sampaio, L., 2010, "On the weaknesses of traditional wave number analysis and its impact in the development of accurate convection discretization", Proceedings of the 13th Brazilian Congress of Thermal Sciences and Engineering (ENCIT).

Tam, C.K.W. and Webb, J.C., 1993, "Dispersion-relation-preserving finite difference schemes for computational acoustics", J. Comput. Phys., vol. 107, no. 2, pp. 262–281.

Tam, C.K.W., Webb, J.C., and Dong, Z., 1993, "A study of the short wave components in computational acoustics", J. Comput. Acoust., vol. 1, no. 1, pp. 1–30.

7. Responsibility notice

The author is the only responsible for the printed material included in this paper